Available online at www.sciencedirect.com
ScienceDirect
Journal of Membrane Science 297 (2007) 190–198
journal of MEMBRANE SCIENCE
www.elsevier.com/locate/memsci

Thermodynamic considerations on the stability of water in Nafion

Gwynn J. Elfring *, Henning Struchtrup

Institute for Integrated Energy Systems, Department of Mechanical Engineering, University of Victoria, PO Box 3055, STN CSC, Victoria, BC V8W 3P6, Canada

Received 8 December 2006; received in revised form 21 March 2007; accepted 24 March 2007
Available online 30 March 2007

Abstract

This work entails modeling the thermodynamic forces contributing to the total free energy of a Nafion membrane to find how liquid water equilibrates and agglomerates inside the membrane. Since the sulfonate acid sites attract water to dissociate, there is a mixture of water and ions within the Nafion membrane. This mixture contributes an entropic term to the free energy of the system which decreases with increasing water content. The hydrophobic Nafion backbone yields a contact angle greater than 90° when in contact with water. This curvature in the surface of the water induces a capillary pressure which can be very high if the size of the agglomeration is small. As the membrane takes on water, polymer chains of the Nafion are stretched and straightened reducing their configurational entropy. Minimizing the free energy under the influence of all these forces at varying pressures and temperatures gives insight into the nature of liquid or vapor filled pores throughout a Nafion membrane. Specifically it indicates a critical pore size in which liquid or vapor is the favorable state.

Keywords: Nafion; Water; Sorption; Equilibrium; Stability

1. Introduction

A fuel cell offers a means to harness the difference in energy when hydrogen and oxygen are combined to form water. In a polymer electrolyte membrane (PEM) fuel cell, a polymer membrane, usually Nafion, separates the two reactants. The hydrogen gas is oxidized on the surface of the electrolyte into protons and electrons. The oxidation reaction is catalyzed by the presence of platinum particles. The membrane acts as an electronic insulator, but allows protons to pass. The electrons are given a path through which they perform work such as powering an electric motor. The reaction is completed as the electrons are diverted to the anode side of the membrane where they react with the protons and oxygen to form water. The level of protonic mobility in the membrane is a function of the level of water content. As water content increases there is a greater interconnection of the liquid phase in the membrane. Bulk water offers extremely high protonic conductivity and as water content increases, Nafion membranes attain more bulk-like transport characteristics [1]. It is therefore critical to examine the nature of water uptake in a Nafion membrane.

Nafion is a sulfonated fluoropolymer; it is comprised of a polytetrafluoroethylene (PTFE) backbone (or matrix), and side chains ending in sulfonic acid groups, see Fig. 1 [2]. The sulfonic acid group, $–SO_3H$, has an affinity for, and dissociates in the presence of water. With increasing water content, the dissociated protons (H^+) become less strongly bound to the $–SO_3^-$ head and therefore facilitate proton conductivity. Since the acid group attracts water in its desire to dissociate, it is hydrophilic. When the acid group dissociates, the proton bonds with a water molecule forming a hydronium ion (H_3O^+) [3]. The liquid water forming around the acid group thus becomes a mixture with the hydronium ion. This mixture affects a change in chemical potential. Therefore, when a Nafion membrane is in the presence of water or water vapor, it draws more water into the membrane to balance the chemical potential. As the membrane takes up water, it swells to accommodate the solvent.

The membrane backbone, however, is hydrophobic. Water confined by hydrophobic surfaces is energetically unfavorable in the liquid state [4]. Together with the elastic forces acting against the swelling, the hydrophobic backbone can be seen to oppose the increasing water content. Eventually an equilibrium state of water content is reached. This equilibrium depends on

* Corresponding author. Tel.: +1 2504725641; fax: +1 2507216323.
E-mail address: gelfring@me.uvic.ca (G.J. Elfring).

0376-7388/$ – see front matter © 2007 Elsevier B.V. All rights reserved.
doi:10.1016/j.memsci.2007.03.044

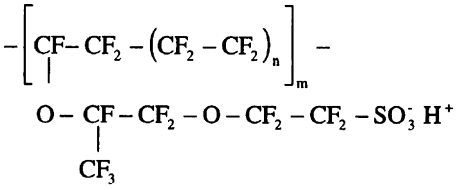

Fig. 1. Nafion chemical structure [2].

whether there is saturated vapor or saturated liquid present at the boundary of the membrane because a vapor/liquid interface provides an additional force opposing water uptake. This difference in the water content of vapor and liquid equilibrated membranes is known as Schroeder's paradox [5,6].

Small-angle X-ray scattering (SAXS) experiments indicate that water tends to collect in small roughly spherical groups in locations which are believed to contain a high concentration of sulfonic acid groups [7]. These spherical clusters were observed to be roughly 3–5 nm in diameter. From these experimental observations, Hsu and Gierke proposed one of the first models for the distribution of water in a Nafion membrane. In this model spherical clusters exist which are 4 nm in diameter and in order to explain the high conductivity of Nafion, Hsu and Gierke postulated that these clusters are connected transient channels of 1–2 nm radius. Weber and Newman refer to the pathways between clusters in Hsu and Gierke's model as 'collapsed channels' [8]. They coin this term because they believe the channel can be expanded and filled by liquid water. In Weber and Newman's model, the channels are regions of the membrane having a low enough concentration of sulfonate heads as to remain hydrophobic. These collapsed channels are assumed to be continuously forming and deforming in ambient conditions due to the movement of free sulfonic acid sites and polymer in the matrix between clusters.

Another early model, by Yeager and Steck, proposed the existence of three distinct regions within the membrane: (A) a hydrophobic matrix, (B) an interfacial zone and, (C) ionic clusters [9]. They propose that the ionic clusters are regions within the membrane with a higher concentration of sulfonate acid sites at which the water will tend to agglomerate. More recently, Kreuer has referred to the hydrated region of a Nafion membrane as "well-connected, even at low degrees of hydration, i.e., there are almost no dead-end pockets and very good percolation" [10]. Fig. 2 shows Kreuer's schematic representation of the microstructure in Nafion derived from SAXS experiments [11]. Kreuer finds that the water distribution forms continuous pathways throughout the membrane. From another recent SAXS study, Gebel concludes that at low levels of hydration one finds inverse micelle clusters of liquid which percolate together with increasing levels of humidity, leading to a structural inversion where the Nafion is seen more as polymer in water than water in polymer [2].

In an analysis on Schroeder's paradox [12] and subsequent work on membrane sorption and transport [13], Choi et al. model the membrane as a series of pores of equal radius. Choi et al. incorporate a model for water uptake in Nafion that was proposed by Futerko and Hsing based on Flory–Huggins theory [14]. The

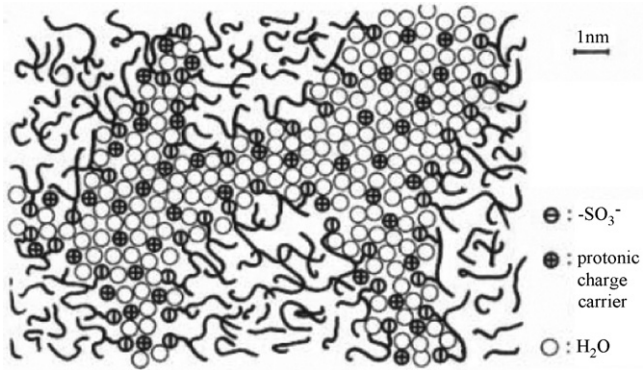

Fig. 2. Microstructure of Nafion according to Kreuer [11].

model fits sorption isotherms to the Flory–Huggins equation by means of the Flory interaction parameter.

The works mentioned consider membrane sorption as a whole. In this work we augment this knowledge by examining the membrane on a microscopic level, in particular the stability of water in a single microscopic pore such as those studied experimentally by Divisek et al. [15]. Proton transport models such as that presented by Paddison et al. [16] focus on water filled cylindrical pores of variable L and r, therefore this work presents a parametric analysis of the wettability of such a cylindrical Nafion micropore. As is done by Gierke and Hsu [7], we model the relevant thermodynamic forces contributing to the total free energy, however we focus on studying the pores prevalent in porous membrane models in order to determine conditions necessary for the stability of liquid water. We plot the free energy of a pore (or channel) filled with liquid of length L against a vapor filled reference state. We determine which state is stable for a given pore radius r_0. We find a critical radius r_c for which liquid is never stable, and show that there exists a critical liquid length $L_{crit}(r)$ for all pore radii larger than r_c. This insight is important because as stated by Paddison et al. [16], it is critical to determine the water-containing phase as it is the region through which conduction occurs. With these results we can also form some intuition regarding the SAXS experimental results prevalent in the literature. We also discuss how this model accounts for a difference in uptake between saturated liquid and saturated vapor equilibrated membranes, and gives support to Weber and Newman's [8] notion that some channels fill or collapse depending on the phase at the boundary.

2. Thermodynamics of sorption

2.1. System

In order to detail the thermodynamic forces which govern the equilibrium state of water in Nafion, we consider a section of Nafion membrane that contains a single pore open at both ends to an environment with a fixed pressure and temperature. We intend to determine which physical conditions are necessary for the agglomeration of liquid water in individual pores. We model these pores, rather idealistically, as cylindrical (see Fig. 3). In a

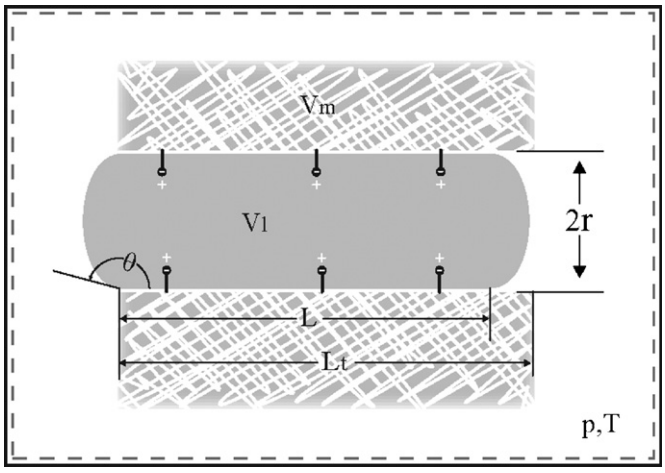

Fig. 3. Pore idealization.

real membrane a tortuous pathway could be seen to be comprised of a series of these ideal pores connected at random.

In this analysis we assume that the liquid agglomeration fills the pore radially and we vary the filling length L to determine stable configurations, alternatively we assume the pore is empty. We do not consider situations in which the radius of the liquid r is smaller than the unstretched radius of the pore r_0.

Moreover, we do not include details on the dissociation reaction of the sulfonate sites with water. This reaction is determined by the law of mass action, outlined in Ref. [12], which governs the behavior of only a few water molecules in the immediate vicinity of the sulfonate group. We only consider an environment at, or near, saturation and therefore we consider these forces equilibrated. Also, while we consider water here, this analysis should be equally applicable to similar solvent systems.

2.1.1. Pores

The surface area of liquid in the pore A_l is composed of the area of the cylindrical portion A_c and the area of the ends A_end:

$$A_\mathrm{l} = A_\mathrm{c} + 2A_\mathrm{end}. \tag{1}$$

A_l is a function of radius r, length L and contact angle θ:

$$A_\mathrm{l} = 2\pi rL + 2\pi r^2 a_\theta, \tag{2}$$

where

$$a_\theta = 2\sec^2\theta[1 - \sin\theta]. \tag{3}$$

Likewise, the volume of liquid in the pore, V_l, is comprised of the volume of the cylindrical region, V_c, and the volume in the curved ends, V_end:

$$V_\mathrm{l} = V_\mathrm{c} + 2V_\mathrm{end}. \tag{4}$$

The explicit expression is

$$V_\mathrm{l} = \pi r^2 L + 2\frac{\pi}{3} r^3 b_\theta, \tag{5}$$

where

$$b_\theta = 2\sec^3\theta[\sin\theta - 1] + \tan\theta. \tag{6}$$

We see (5) with $L = 0$ does not describe an empty pore. It is important therefore, to note that in this description, even when the length L of the liquid agglomeration is zero, V_l refers to a 'lentil' of volume $2V_\mathrm{end}$, due to the curved ends.

2.2. Surface free energy

The surface energy F_s for a liquid agglomeration of length L in a cylindrical pore of total length L_t is given by

$$F_\mathrm{s} = \gamma_\mathrm{sv} 2\pi r(L_\mathrm{t} - L) + \gamma_\mathrm{sl} 2\pi rL + 2\gamma_\mathrm{lv}\pi r^2 a_\theta, \tag{7}$$

where γ_sv, γ_sl and γ_lv are the interfacial tensions of the solid–vapor, solid–liquid and liquid–vapor interfaces, respectively [17]. Using Young's equation [18]:

$$\frac{\gamma_\mathrm{sv} - \gamma_\mathrm{sl}}{\gamma_\mathrm{lv}} = \cos\theta \tag{8}$$

to relate the interfacial tensions to the contact angle with the membrane, we can rewrite (7) as

$$F_\mathrm{s} = \gamma_\mathrm{sv} 2\pi rL_\mathrm{t} - 2\pi rL\gamma_\mathrm{lv}\cos\theta + 2\gamma_\mathrm{lv}\pi r^2 a_\theta. \tag{9}$$

2.3. The nature of equilibrium

From the first and second laws of thermodynamics, for a system with fixed external pressure and temperature, one finds

$$\frac{\mathrm{d}\mathcal{G}}{\mathrm{d}t} \leq 0, \tag{10}$$

where $\mathcal{G} = U - TS + pV$ is the total free energy of the system. This states that the total free energy of the system decreases in time, such that $\mathcal{G}$ assumes a minimum in equilibrium. We therefore must include all contributions to free energy in order to determine equilibrium conditions. We follow a formal approach laid out by Morro and Müller [19] for the case of polyelectrolyte gels in a closed system. Writing out all contributions to $\mathcal{G}$ in terms of the Helmholtz free energy in the unmixed state $F_\alpha = f_\alpha(v)m_\alpha$ and the entropy of mixing $S_{\alpha,\mathrm{mix}}$ we obtain

$$\begin{aligned}\mathcal{G} = {} & F_\mathrm{l} + S_{\mathrm{l,mix}} + F_\mathrm{p} + S_{\mathrm{p,mix}} + F_\mathrm{v} + F_\mathrm{s} + F_\mathrm{m} \\ & + p(V_\mathrm{l} + V_\mathrm{p} + V_\mathrm{v} + V_\mathrm{m}).\end{aligned} \tag{11}$$

The subscripts $\alpha = \mathrm{l}$, p, v, s, and m refer to the liquid, protons, vapor, surface and membrane, respectively. Since the membrane is phase-separated there is no mixing of the polymer chains with the liquid in the pore. With the entropy of mixing given explicitly (11) yields

$$\begin{aligned}\mathcal{G} = {} & [f_\mathrm{l} + R_\mathrm{l}T\ln a_\mathrm{l}]m_\mathrm{l} + [f_\mathrm{p} + R_\mathrm{p}T\ln a_\mathrm{p}]m_\mathrm{p} + f_\mathrm{p}^0 m_\mathrm{p}^0 + f_\mathrm{v}m_\mathrm{v} \\ & + F_\mathrm{s} + F_\mathrm{m} + p(V_\mathrm{l} + V_\mathrm{p} + V_\mathrm{p}^0 + V_\mathrm{v} + V_\mathrm{m}).\end{aligned} \tag{12}$$

Here, R denotes the gas constant and a is the activity of the mixture of liquid molecules and protons. The protons within the liquid mixture are referred to by m_p and V_p while the protons outside the liquid boundary are denoted by m_p^0 and V_p^0. The total number of protons in the pore:

$$m_\mathrm{p}^\mathrm{T} = m_\mathrm{p} + m_\mathrm{p}^0 \tag{13}$$

is constant. Therefore, with the assumption that the protons are incompressible, the total volume of the protons stays constant. The activity a is defined as

$$a = \gamma^{\mathrm{a}} X, \tag{14}$$

where γ^{a} is the activity coefficient and X is the mole fraction in the mixture:

$$X_{\mathrm{l}} = \frac{N_{\mathrm{l}}}{N_{\mathrm{l}} + N_{\mathrm{p}}}. \tag{15}$$

By means of (14) the free energy of the system can be rewritten as

$$\begin{aligned}\mathcal{G} = {} & [F_{\mathrm{l}} + R_{\mathrm{l}} T \ln X_{\mathrm{l}}] m_{\mathrm{l}} + [f_{\mathrm{p}} + R_{\mathrm{p}} T \ln X_{\mathrm{p}}] m_{\mathrm{p}} + f_{\mathrm{p}}^0 m_{\mathrm{p}}^0 \\ & + f_{\mathrm{v}} m_{\mathrm{v}} + F_{\mathrm{s}} + F_{\mathrm{m}} + p(V_{\mathrm{l}} + V_{\mathrm{p}} + V_{\mathrm{p}}^0 + V_{\mathrm{v}} + V_{\mathrm{m}}) \\ & + R_{\mathrm{u}} T (N_{\mathrm{l}} \ln \gamma_{\mathrm{l}}^{\mathrm{a}} + N_{\mathrm{p}} \ln \gamma_{\mathrm{p}}^{\mathrm{a}}).\end{aligned} \tag{16}$$

The last term represents the excess Gibbs free energy of mixing G^{E}, or the energy difference with respect to ideal mixing. This can be expressed in terms of a Flory interaction parameter χ [20], as

$$\frac{G^{\mathrm{E}}}{R_{\mathrm{u}} T} = (N_{\mathrm{l}} \ln \gamma_{\mathrm{l}}^{\mathrm{a}} + N_{\mathrm{p}} \ln \gamma_{\mathrm{p}}^{\mathrm{a}}) = N_{\mathrm{p}} X_{\mathrm{l}} \chi_{\mathrm{pl}}(T). \tag{17}$$

With (17), (16) can be written as

$$\begin{aligned}\mathcal{G} = {} & [f_{\mathrm{l}} + R_{\mathrm{l}} T \ln X_{\mathrm{l}}] m_{\mathrm{l}} + [f_{\mathrm{p}} + R_{\mathrm{p}} T \ln X_{\mathrm{p}}] m_{\mathrm{p}} + f_{\mathrm{p}}^0 m_{\mathrm{p}}^0 \\ & + f_{\mathrm{v}} m_{\mathrm{v}} + F_{\mathrm{s}} + F_{\mathrm{m}} + p(V_{\mathrm{l}} + V_{\mathrm{p}} + V_{\mathrm{p}}^0 + V_{\mathrm{v}} + V_{\mathrm{m}}) \\ & + R_{\mathrm{u}} T N_{\mathrm{p}} X_{\mathrm{l}} \chi_{\mathrm{pl}}.\end{aligned} \tag{18}$$

For equilibrium, we must minimize $\mathcal{G}$ with respect to the variables that change in time: the mass of liquid in the pore m_{l}, the mass of vapor m_{v}, the volume of vapor V_{v}, and the volume of liquid V_{l}. Since we are considering a closed system, the total mass stays constant:

$$m_{\mathrm{w}} = m_{\mathrm{l}} + m_{\mathrm{v}} = \text{const}. \tag{19}$$

Hence, the conditions for equilibrium are

$$\frac{\partial \mathcal{G}}{\partial m_{\mathrm{l}}} = \frac{\partial \mathcal{G}}{\partial V_{\mathrm{l}}} = \frac{\partial \mathcal{G}}{\partial V_{\mathrm{v}}} = 0. \tag{20}$$

Each of the equations in (20) reveals further information about equilibrium.

Minimizing the total free energy with respect to the mass of liquid, m_{l}, yields

$$\begin{aligned}\frac{\partial \mathcal{G}}{\partial m_{\mathrm{l}}} = {} & f_{\mathrm{l}} + R_{\mathrm{l}} T \ln X_{\mathrm{l}} + m_{\mathrm{l}} \frac{\partial f_{\mathrm{l}}}{\partial v_{\mathrm{l}}} \frac{\partial v_{\mathrm{l}}}{\partial m_{\mathrm{l}}} + m_{\mathrm{l}} R_{\mathrm{l}} T \frac{\partial \ln X_{\mathrm{l}}}{\partial m_{\mathrm{l}}} \\ & + m_{\mathrm{p}} R_{\mathrm{p}} T \frac{\partial \ln X_{\mathrm{p}}}{\partial m_{\mathrm{l}}} - f_{\mathrm{v}} - m_{\mathrm{v}} \frac{\partial f_{\mathrm{v}}}{\partial v_{\mathrm{v}}} \frac{\partial v_{\mathrm{v}}}{\partial m_{\mathrm{v}}} \\ & + m_{\mathrm{p}} R_{\mathrm{p}} T \chi_{\mathrm{pl}} \frac{\partial X_{\mathrm{l}}}{\partial m_{\mathrm{l}}} = 0.\end{aligned} \tag{21}$$

With the Gibbs–Duhem relation and Maxwell relations this simplifies to

$$g_{\mathrm{l}} + R_{\mathrm{l}} T [\ln X_{\mathrm{l}} + \chi_{\mathrm{pl}} X_{\mathrm{p}}^2] = g_{\mathrm{l}} + R_{\mathrm{l}} T \ln a_{\mathrm{l}} = g_{\mathrm{v}} \tag{22}$$

with the Gibbs free energy $g_{\mathrm{l}} = f_{\mathrm{l}} + p_{\mathrm{l}} V_{\mathrm{l}}$. Eq. (22) states the familiar result that the chemical potentials of the liquid and vapor are equal in equilibrium.

Minimizing the total free energy with respect to the volume of the vapor yields

$$\frac{\partial \mathcal{G}}{\partial V_{\mathrm{v}}} = m_{\mathrm{v}} \frac{\partial f_{\mathrm{v}}}{\partial v_{\mathrm{v}}} \frac{\partial v_{\mathrm{v}}}{\partial V_{\mathrm{v}}} + p = 0. \tag{23}$$

This reduces to

$$-p_{\mathrm{v}} + p = 0, \tag{24}$$

which states that the pressure of the vapor is equal to the pressure imposed on the system.

Minimizing the total Gibbs free energy with respect to the volume of the liquid gives

$$\begin{aligned}\frac{\partial \mathcal{G}}{\partial V_{\mathrm{l}}} = {} & m_{\mathrm{l}} \frac{\partial f_{\mathrm{l}}}{\partial v_{\mathrm{l}}} \frac{\partial v_{\mathrm{l}}}{\partial V_{\mathrm{l}}} + m_{\mathrm{l}} R_{\mathrm{l}} T \frac{\partial \ln X_{\mathrm{l}}}{\partial V_{\mathrm{l}}} + m_{\mathrm{p}} R_{\mathrm{p}} T \frac{\partial \ln X_{\mathrm{p}}}{\partial V_{\mathrm{l}}} + f_{\mathrm{p}} \frac{\partial m_{\mathrm{p}}}{\partial V_{\mathrm{l}}} \\ & + R_{\mathrm{p}} T \ln X_{\mathrm{p}} \frac{\partial m_{\mathrm{p}}}{\partial V_{\mathrm{l}}} + f_{\mathrm{p}}^0 \frac{\partial m_{\mathrm{p}}^0}{\partial V_{\mathrm{l}}} + p + \frac{\partial F_{\mathrm{s}}}{\partial V_{\mathrm{l}}} + \frac{\partial F_{\mathrm{m}}}{\partial V_{\mathrm{l}}} \\ & + R_{\mathrm{p}} T \chi_{\mathrm{pl}} \left[X_{\mathrm{l}} \frac{\partial m_{\mathrm{p}}}{\partial V_{\mathrm{l}}} + m_{\mathrm{p}} \frac{\partial X_{\mathrm{l}}}{\partial V_{\mathrm{l}}} \right] = 0.\end{aligned} \tag{25}$$

Simplifying with (13) and the Gibbs-Duhem relation leads to

$$\begin{aligned}\frac{\partial \mathcal{G}}{\partial V_{\mathrm{l}}} = {} & \frac{\partial f_{\mathrm{l}}}{\partial v_{\mathrm{l}}} + [f_{\mathrm{p}} - f_{\mathrm{p}}^0 + R_{\mathrm{p}} T (\ln X_{\mathrm{p}} + \chi_{\mathrm{pl}} X_{\mathrm{l}}^2)] \frac{\partial m_{\mathrm{p}}}{\partial V_{\mathrm{l}}} + p \\ & + \frac{\partial F_{\mathrm{s}}}{\partial V_{\mathrm{l}}} + \frac{\partial F_{\mathrm{m}}}{\partial V_{\mathrm{l}}} = 0.\end{aligned} \tag{26}$$

The pressure in the mixture results from the derivative:

$$\frac{\partial f_{\mathrm{l}}}{\partial v_{\mathrm{l}}} = -p_{\mathrm{mix}}.$$

We define the surface pressure:

$$p_{\mathrm{s}} = \frac{\partial F_{\mathrm{s}}}{\partial V_{\mathrm{l}}}, \tag{27}$$

which is due to the change in surface free energy when the liquid volume changes, and the membrane pressure:

$$p_{\mathrm{m}} = \frac{\partial F_{\mathrm{m}}}{\partial V_{\mathrm{l}}}, \tag{28}$$

which is due to the change of membrane free energy with a change in liquid volume. We also define a proton pressure:

$$\begin{aligned}p_{\mathrm{p}} = {} & [f_{\mathrm{p}} - f_{\mathrm{p}}^0 + R_{\mathrm{p}} T (\ln X_{\mathrm{p}} + \chi_{\mathrm{pl}} X_{\mathrm{l}}^2)] \frac{\partial m_{\mathrm{p}}}{\partial V_{\mathrm{l}}} \\ = {} & [f_{\mathrm{p}} - f_{\mathrm{p}}^0 + R_{\mathrm{p}} T \ln a_{\mathrm{p}}] \frac{\partial m_{\mathrm{p}}}{\partial V_{\mathrm{l}}},\end{aligned} \tag{29}$$

which is the energy required to add more protons to the mixture as the boundary of V_l expands. We can thus rewrite (26) as

$$p_{mix} = p + p_s + p_m + p_p, \tag{30}$$

which yields the pressure of the liquid/proton mixture, which is a function of the energies of the surface, membrane and protons in the mixture.

We now can substitute the conditions of mechanical equilibrium, (24) and (30), into (12), replace the specific Helmholtz free energy f with the Gibbs free energy g, and use (19) to find

$$\begin{aligned}\mathcal{G} = {} & [g_l + R_l T \ln X_l]m_l + [g_p + R_p T(\ln X_p + X_l\chi_{pl})]m_p \\ & + g_p^0 m_p^0 + g_v m_w - g_v m_l + F_m + pV_m \\ & - (p_s + p_m + p_p)(V_l + V_p) + F_s.\end{aligned} \tag{31}$$

Since we take vapor as an ideal gas and assume that liquid water is incompressible, we can write

$$\begin{aligned}g_v(p_v) &= g_v(p_{sat}) + R_v T \ln\left(\frac{p}{p_{sat}}\right) \\ &= g_l(p) + (p_{sat} - p)v_l + R_v T \ln\left(\frac{p}{p_{sat}}\right)\end{aligned} \tag{32}$$

and

$$g_l(p_{mix}) = g_l(p + p_s + p_m + p_p) = g_l(p) + v_l(p_s + p_m + p_p). \tag{33}$$

We use the same argument for the protons and substitute back into (31) with $P_r = p/P_{sat}$, $R_l = R_v = R_w$, and $X_p = 1 - X_l$, to obtain

$$\begin{aligned}\mathcal{G} = {} & \left[(p - p_{sat}) + \frac{R_w T}{v_l}\ln\left(\frac{X_l}{p_r}\right)\right] V_l \\ & + [g_p(p) + R_p T(\ln(1 - X_l) + X_l\chi_{pl})]m_p \\ & + g_p^0 m_p^0 + g_v m_v + F_m + pV_m + F_s.\end{aligned} \tag{34}$$

We see that the pressure within the pore is no longer explicit, but remains implicit as defined by the equilibrium conditions.

We introduce as a reference state, the free energy of a vapor filled pore:

$$\mathcal{G}^0 = g_v m_w + g_p^0(p)m_p^T + F_m^0 + pV_m^0 + F_s^0. \tag{35}$$

Subtracting this reference from (34) gives

$$\begin{aligned}\mathcal{G} - \mathcal{G}^0 = {} & \left[(p - p_{sat}) + \frac{R_w T}{v_l}\ln\left(\frac{X_l}{p_r}\right)\right] V_l \\ & + [g_p(p) - g_p^0(p) + R_p T(\ln(1 - X_l) + X_l\chi_{pl})]m_p \\ & + F_m - F_m^0 + p(V_m - V_m^0) + F_s - F_s^0.\end{aligned} \tag{36}$$

2.4. Cylindrical system

We now impose the cylindrical geometry of the pores. The mass of the protons may be expressed through the surface density of sulfonate sites S_p (which are assumed to be ionized) and the surface area of the unstretched pore in contact with liquid as

$$m_p = M_p S_p 2\pi r_0 L, \tag{37}$$

where M_p is the molar mass. The reference state is vapor filled and therefore remains at an unstretched radius r_0. The surface free energy of the reference state is therefore given simply by

$$F_s^0 = \gamma_{sv} 2\pi r_0 L_t.$$

Substituting m_p, V_l, F_s, F_s^0 into (36), one obtains

$$\begin{aligned}\mathcal{G} - \mathcal{G}^0 = {} & \left[(p - p_{sat}) + \frac{R_w T}{v_l}\ln\left(\frac{X_l}{p_r}\right)\right]\left(\pi r^2 L + \frac{2\pi r^3}{3}b_\theta\right) \\ & + [g_p(p) - g_p^0(p) + R_p T(\ln(1 - X_l) + X_l\chi_{pl})] \\ & \times 2\pi r_0 L M_p S_p + (F_m - F_m^0) + p(V_m - V_m^0) \\ & + \gamma_{sv} 2\pi(r - r_0)L_t - 2\pi r L\gamma_{lv}\cos\theta + 2\gamma_{lv}\pi r^2 a_\theta.\end{aligned} \tag{38}$$

The number of ions in a pore is

$$N_p = A_c S_p = 2\pi r_0 L S_p \tag{39}$$

and the number of water molecules in the pore is

$$N_l = \frac{\rho_w}{M_w}V_l = \frac{\rho_w}{M_w}(\pi r^2 L + 2\pi r^3 b_\theta). \tag{40}$$

The mole ratio of liquid water is then

$$X_l = \frac{r^2 L + 2r^3 b_\theta}{2\beta r_0 L + r^2 L + 2r^3 b_\theta}, \tag{41}$$

where $\beta = S_p M_w/\rho_w$.

By subtracting the free energy of a vapor filled pore, we know that if the difference $\mathcal{G} - \mathcal{G}^0$ is negative, then the free energy of the vapor state is lower and therefore the vapor filled state is more stable. Subtraction of $\mathcal{G}^0$ also conveniently eliminates various constants if $r = r_0$, which occurs when we do not consider membrane stretching.

For the vapor filled reference state, we assume that a number of water molecules have reacted with the sulfonate site. The number of these waters is evaluated through the law of mass action, the details of which may be found, for instance, in Ref. [12]. These waters are strongly bound and exist regardless of whether a liquid phase fills the pore. For the purpose of this work, we assume that the subsequent waters forming the liquid phase do not significantly alter the free energy of the protons, therefore the $g_p(p) - g_p^0(p)$ term is negligible.

The change in the free energy of the membrane describes elastic forces and only occurs when the membrane is stretched to $r > r_0$, to allow more water into the pore. We assume that when the membrane stretches, the volume of the membrane backbone itself remains constant, $V_m = V_m^0$ for all r. The change in volume of the system is therefore due to the increasing water volume. For an isotropic material, Flory [20] finds the change

in free energy:

$$F_m - F_m^0 = \Delta F_{el} = \frac{kTv_e}{2}[3\alpha^{3/2} - 3 - \ln\alpha] \tag{42}$$

where k is the Boltzmann constant, v_e the elastically effective number of chains in the polymer network and $\alpha = V/V^0$ where V^0 is the volume of the unstretched pore. We use the effective number of chains because polymers other than Nafion may contain crosslinks; evidence of the effect of crosslinking on sorption in polymide membranes is detailed in Ref. [21]. A slight modification of (42) is used by Morro and Müller [19]. More recent derivations of the free energy due to membrane stretching can be found in Refs. [22,23], however, the applicability of any one of these derivations for the elastic energy is debatable when a single phase-separated microscopic pore is considered. For completeness we show (42) for a cylindrical pore of unstretched radius r_0, with (38) which yields the free energy in L and r:

$$\begin{aligned}\mathcal{G} - \mathcal{G}^0 = &\left[(p - p_{sat}) + \frac{R_w T}{v_l}\ln\left(\frac{r^2L + 2r^3b_\theta}{p_r[2\beta r_0 L + r^2L + 2r^3b_\theta}\right)\right] \\ &\times \left(\pi r^2 L + \frac{2\pi r^3}{3}b_\theta\right) \\ &+ R_u T\left[\ln\left(1 - \frac{r^2L + 2r^3b_\theta}{2\beta r_0 L + r^2L + 2r^3b_\theta}\right)\right. \\ &\left.+ \frac{r^2L + 2r^3b_\theta}{2\beta r_0 L + r^2L + 2r^3b_\theta}\chi_{pl}\right] 2\pi r_0 L S_p \\ &+ \frac{kTv_e}{2}\left[3\left(\frac{r}{r_0}\right)^3 - 3 - 2\ln\left(\frac{r}{r_0}\right)\right] \\ &+ \gamma_{sv}2\pi(r - r_0)L_t - 2\pi r L\gamma_{lv}\cos\theta + 2\gamma_{lv}\pi r^2 a_\theta.\end{aligned} \tag{43}$$

2.4.1. Capillary pressure

We briefly consider the surface pressure in a cylindrical pore. Substituting our definition of F_s (9) into (27) yields

$$p_s = \frac{\partial F_s}{\partial V_l} = \frac{\partial}{\partial V_l}[\gamma_{sv}2\pi r L_t - 2\pi r L\gamma_{lv}\cos\theta + 2\gamma_{lv}\pi r^2 a_\theta]. \tag{44}$$

If r is constrained to r_0, and the liquid volume V_l can grow in L as the column of water extends down the pore, then

$$p_s = \frac{\partial F_s}{\partial V_l} = \frac{\partial F_s}{\partial L}\frac{\partial L}{\partial V_l} = -\frac{2\gamma_{lv}\cos\theta}{r_0}, \tag{45}$$

which is the classical Laplace equation for capillary pressure.

3. Finding minima

Our purpose is to find thermodynamically stable pore configurations for the presence of liquid agglomerations. In this section we minimize the total free energy of the system in order to study which situations are conducive to liquid or vapor filled regions of a Nafion membrane. Since in our formulation we subtract the constant free energy of a vapor filled pore, $\mathcal{G}^0$, we know that if

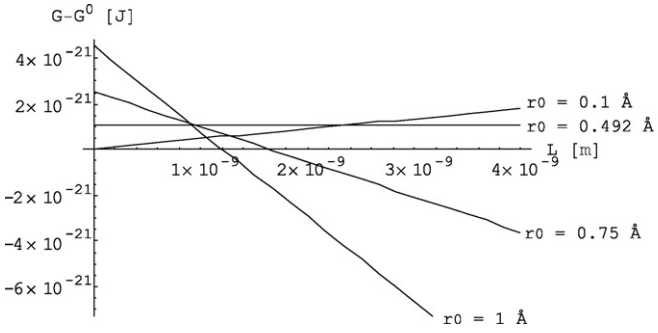

Fig. 4. Free energy vs. L ($r_0 = 0.1$ Å:0.1 Å).

$\mathcal{G} - \mathcal{G}^0$ is negative then liquid is favorable. If, on the other hand, $\mathcal{G} - \mathcal{G}^0$ is positive, then free energy of vapor is lower and thus more stable. If liquid is favorable, $\mathcal{G} - \mathcal{G}^0$ will assume a negative minimum.

3.1. Unstretched pores

In the following we consider unstretched pores to determine which regions of the membrane would contain liquid water in equilibrium, at a given pressure and temperature. When the pore is not stretched $r = r_0$ and (43) becomes

$$\begin{aligned}\mathcal{G} - \mathcal{G}^0 = 2\pi r_0 L\left\{\frac{r_0}{2}\frac{R_w T}{v_l}\ln\left(\frac{X_l}{p_r}\right) + R_u T[\ln(1 - X_l)\right. \\ \left. + X_l\chi_{pl}]S_p - \gamma_{lv}\cos\theta\right\} + f_{end}.\end{aligned} \tag{46}$$

The last term is an abbreviation for

$$f_{end} = \left[(p - p_{sat}) + \frac{R_w T}{v_l}\ln\left(\frac{X_l}{p_r}\right)\right]\frac{2\pi r_0^3}{3}b_\theta + 2\gamma_{lv}\pi r_0^2 a_\theta; \tag{47}$$

it represents the end effects, which is the energy of the lentil that is present when $L = 0$.

To compute $\mathcal{G} - \mathcal{G}^0$ we use a value of $\theta = 98^\circ$ taken from Zawodzinski et al. [24], measured at $p_r = 1$. Zawodzinski et al. find that θ varies with water content, generally given by $\lambda = H_2O/SO_3H$. This variation is fairly substantial, with $\theta = 116^\circ$ for $\lambda = 0$, while the above value is for $\lambda = 14$. We are primarily concerned with hydration near saturation, therefore we hold $\theta = 98^\circ$ constant, however, this measurement perhaps couples the attraction of the protons with the repulsion of the backbone and should be investigated. As in Ref. [25] we set $\chi_{pl} = 0$, which gives ideal mixing, for lack of a detailed data set. To compute the surface density of sulfonate sites we use $s_p = (\bar{V}_m S)^{-1}$, where $\bar{V}_m$ is the specific molar volume of the membrane and S is the specific pore surface area. We take the values, $\bar{V}_m = 537\,cm^2/mol$ and $S = 210\,m^2/cm^3$ for Nafion 117 from Refs. [13,15], respectively. T is taken to be 300 K.

Fig. 4 shows $\mathcal{G} - \mathcal{G}^0$ against L for various pore radii. We see that the free energy is essentially independent of L at critical pore radius of $r_c = 0.492$ Å. For all pores wider than this, growth of a liquid agglomeration reduces the free energy of

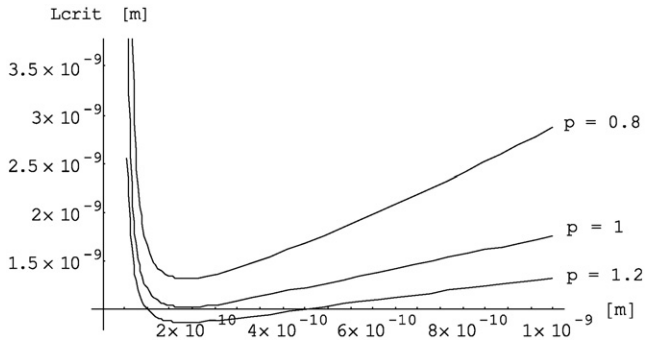

Fig. 5. L_{crit} vs. r_0 ($p_r = 0.8{:}1.2$).

the system. However, L must be larger than a certain critical value $L_{crit}(r)$ for liquid stability. Stability for liquid occurs when $\mathcal{G} - \mathcal{G}^0$ is negative, so that the free energy of liquid is lower than that of vapor. Therefore $L_{crit}(r)$ is obtained as the solution of $\mathcal{G} - \mathcal{G}^0$. Pores must be longer than the critical length for a certain pore radius, $L_t > L_{crit}(r)$, in order to fill with liquid. If so, they will fill completely since then the minimum of $\mathcal{G} - \mathcal{G}^0$ is obtained for L as large as possible. If the pore fills completely, it will begin to stretch radially until balanced by the elastic energy.

Fig. 5 shows $L_{crit}(r)$ for various pressure ratios p_r. For very narrow pores, with radii smaller than about $r_0 = 0.1$ nm, liquid stability is unlikely, since the critical length required for a pore becomes very large. This is because entropic effects, which favor liquid, scale with volume, while the surface forces, which favor vapor, scale with surface area. In pores with very small radii, the surface forces dominate. Experimentally measured 'clusters' of radii 5–25 Å, observed in various diffraction and microscopic studies [26], are certainly within the calculated range of stability.

Fig. 5 also indicates that the stability of liquid depends on pressure. The effects of the pressure ratio p_r, especially under-saturation ($p_r < 1$), are much stronger for wider pores, where the entropic effects begin to dominate. This indicates why the water content in Nafion is drastically reduced in under-saturated environments, as shown in Ref. [27]. The interconnection of liquid pathways sharply decreases due to under-saturation, which accounts for the drastic reduction in conductivity of the membrane in under-saturated states [1].

Recall that we only consider pores where liquid fills the whole pore radius, and consider variations in L which would lead to a lower free energy than the vapor filled state. We do not consider liquid agglomeration of radii lower than the unstretched pore diameter, $r < r_0$. These situations are unlikely to be stable due to the high interfacial energy between liquid and vapor.

The above observations concern equilibrium states. Liquid agglomerations have to transition through unstable configurations when filling a pore to reach a final stable state. In a similar analogy, a droplet of rain in the atmosphere transitions to a critical radius in which growth is favorable, through smaller unstable radii, with the help of a particle of dust [28]. The intermediate non-equilibrium states in the membrane are certainly interesting but are not considered here.

3.1.1. Schroeder's paradox

In a saturated liquid environment the membrane is bounded by liquid water, therefore the end effects, which are due to the liquid–vapor interface, are not present in a liquid filled pore. Thus, in (46) f_{end} goes to zero and we are left with

$$\mathcal{G} - \mathcal{G}^0 = 2\pi r_0 L \left\{ \frac{r_0}{2} \frac{R_w T}{v_l} \ln\left(\frac{X_l}{p_r}\right) + R_u T[\ln(1 - X_l) + X_l \chi_{pl}] S_p - \gamma_{lv} \cos\theta \right\}. \tag{48}$$

The mole ratio becomes

$$X_l = \frac{r_0 \xi}{2 + r_0 \xi}, \tag{49}$$

where $\xi = \beta^{-1}$.

We see that the total free energy (48) is linear in L. The solution of

$$\frac{r_0}{2} \frac{R_w T}{v_l} \ln\left(\frac{r_0 \xi}{p_r[2 + r_0 \xi]}\right) + R_u T \left[\ln\left(1 - \frac{r_0 \xi}{2 + r_0 \xi}\right) + \left(\frac{r_0 \xi}{2 + r_0 \xi}\right) \chi_{pl}\right] S_p - \gamma_{lv} \cos\theta = 0, \tag{50}$$

for r_0 yields a critical radius of $r_c = 0.0056$ Å, with the constants given. If $r_0 > r_c$, (48) has a minimum at the largest possible value of L, that is when $L = L_t$, and if $r_0 > r_c$, the minimum occurs at the smallest possible value of L, that is when $L = 0$. It is important to note that if $L = 0$, we have an evaporation of the liquid in the pore which would create a liquid–vapor interface at the bounds leading, therefore, to a critical radius that is even smaller. The critical radius found is however negligibly small already, in a range where the continuum nature of this analysis is no longer valid. We do see very clearly however, a drastic reduction in the criteria necessary for the stability of liquid, therefore there are some pores which were vapor filled in a saturated vapor environment which would fill with liquid when equilibrated with saturated liquid in agreement with the predictions of Weber and Newman [8].

A pore may not have contact with the environment at both ends. Fig. 6 shows the difference in stability requirements if just one liquid–vapor interface is eliminated, occurring if the pore bounds the saturated liquid environment at just one end. The

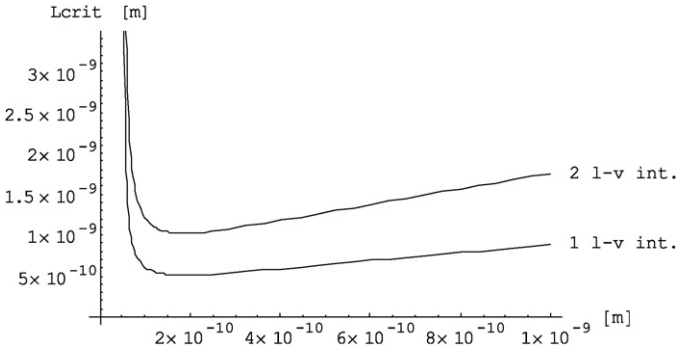

Fig. 6. Effects of the liquid–vapor interface.

critical length for this case is considerably smaller than for the case where both ends are in contact with vapor.

We see in this analysis, that the elimination of end effects reduces the criteria for liquid stability and therefore dictates that Nafion absorb significantly more water in a saturated liquid environment. It is important to note however that the phenomenon of Schroeder's paradox is not necessarily coupled with a porous structure as detailed in Ref. [6]. We do however see here that given a porous structure with can expect a considerable difference in sorption given a change in the phase at the boundary.

3.2. Pore stretching

Liquid growth in L is constrained to boundary minima, at either $L = L_t$ or $L = 0$. A full pore will, however, begin to stretch, to $r > r_0$, in order to take on more water. Nafion is known to stretch significantly in the presence of water. The pore comes to an equilibrium point in r when the change in free energy of the membrane due to stretching balances the entropic desire to take on more water. We do not consider the deformation of the pore from its initial radius in this work as it does not determine in which regions of a membrane liquid might be stable. A future work will consider the deformation of individual pores.

4. Conclusion

The conductivity of a Nafion membrane is dramatically affected by the amount of water that is sorbed by the membrane. It is therefore important to consider the fundamental thermodynamic forces affecting sorption. The majority of literature focuses on modeling the membrane as a whole to consider sorption. This work, however, examined a single microscopic pore to determine what thermodynamic forces are present and whether liquid water or vapor will equilibrate. This is important since many proton transport models are based on the assumption of water filled cylindrical pores. Based on a simple thermodynamic model it was shown that there exists a critical pore radius below which water is unstable. Moreover, we found a critical length for any pore size greater than the critical radius; below the critical length, a pore cannot be filled. This model is also used to show how pressure, relative to saturation, affects liquid agglomeration. This work therefore documents criteria necessary for the permeation of the liquid phase within a Nafion membrane.

Our model was also used to study how thermodynamic forces change depending on whether there is saturated liquid or vapor at the bounds of the membrane. The results shows that in a saturated liquid environment much smaller pores will fill with liquid. This is useful in understanding how Nafion sorbs so much more water when in saturated liquid as opposed to saturated vapor.

Acknowledgment

This research was supported by the Natural Sciences and Engineering Research Council (NSERC).

Nomenclature

a	activity
a_θ	end area function
A	area (m^2)
A_c	area of cylinder (m^2)
A_{end}	area of end (m^2)
b_θ	end volume function
f	specific Helmholtz free energy (J/kg)
f_{end}	energy of ends (J)
F	Helmholtz free energy
F_{el}	elastic energy of membrane (J)
g	specific Gibbs free energy (J/kg)
G^E	Gibbs excess free energy (J)
$\mathcal{G}$	total free energy of the system (J)
k	Boltzmann constant (1.381×10^{-23} J/K)
L	length of liquid agglomeration (m)
L_t	length of pore (m)
m	mass (kg)
m_p^T	total mass of protons (kg)
M	molar mass (kg/mol)
N	number of molecules
p	pressure (Pa)
p_r	pressure ratio
p_{sat}	saturation pressure (Pa)
P_{mix}	pressure of liquid water and proton mixture (Pa)
r	radius of liquid agglomeration (m)
r_0	unstretched pore radius (m)
r_c	critical pore radius for the stability of liquid water (m)
R	specific gas constant ($J\,kg^{-1}\,K^{-1}$)
R_u	universal gas constant ($8.314\,J\,mol^{-1}\,K^{-1}$)
S_{mix}	entropy of mixing ($J\,kg^{-1}\,K^{-1}$)
S_p	surface density of protons (m^{-2})
t	time (s)
T	temperature (K)
v	specific volume (m^3/kg)
V	volume (m^3)
V_c	volume of cylinder (m^3)
V_{end}	volume of end (m^3)
X	mole fraction

Greek symbols

α	volume ratio of stretched to unstretched pores
β	$S_p M_w/\rho_w$ (m^{-2})
γ	interfacial tension (J/m^2)
γ^a	activity coefficient
θ	contact angle
λ	water content
μ	chemical potential (J/kg)
ν_e	effective number of chains in the polymer network
ξ	β^{-1} (m^2)
ρ	mass density (kg/m^3)
χ	interaction parameter

Subscripts

l	liquid
lv	liquid–vapor
m	membrane
p	proton
s	surface
sl	solid–liquid
sv	solid–vapor
v	vapor
w	water

Superscript

0	unstretched vapor filled reference state

References

[1] J. Fimrite, H. Struchtrup, N. Djilali, Transport Phenomena in Polymer Electrolyte Membranes. I. Modeling Framework, J. Electrochem. Soc. 152 (2005) A1804–A1814.

[2] G. Gebel, Structural evolution of water swollen perfluorosulfonated ionomers from dry membrane to swollen, Polymer 41 (2000) 5829–5838.

[3] A. Zecchina, F. Geobadlo, G. SPoto, S. Bordiga, G. Ricchiardi, R. Buzzoni, G. Petrini, Interaction of H_2O, CH_3OH, $(CH_3)(2)O$, CH_3CN, and pyridine with the superacid perfluorosulfonic membrane Nafion—an IR and Raman study, J. Phys. Chem. 99 (1995) 11937.

[4] H.K. Christenson, P.M. Claesson, Cavitation and the interaction between macroscopic hydrophobic surfaces, Science 239 (1988) 390–392.

[5] P. Schroeder, Uber Erstarrungs-und Quellungserscheinungen von Gelatine, Z. Phys. Chem. 45 (1903) 57.

[6] C. Vallieres, D. Winkelmann, D. Roizard, E. Favre, P. Scharfer, M. Kind, On Schroeder's paradox, J. Membr. Sci. 278 (2006) 357–364.

[7] T.D. Gierke, W.Y. Hsu, Ion-transport and clustering in Nafion perfluorinated membranes, J. Membr. Sci. 13 (1983) 307–326.

[8] A.Z. Weber, J. Newman, Transport in polymer–electrolyte membranes I. Physical model, J. Electrochem. Soc. 150 (2003) A1008–A1015.

[9] H.L. Yeager, A. Steck, Cation and water diffusion in Nafion ion exchange membranes: influence of polymer structure, J. Electrochem. Soc. 128 (1981) 1880–1884.

[10] K.D. Kreuer, S.J. Paddison, E. Spohr, M. Schuster, Transport in proton conductors for fuel-cell applications: simulations, elementary reactions, and phenomenology, Chem. Rev. 104 (2004) 4637–4678.

[11] K.D. Kreuer, On the development of proton conducting polymer membranes for hydrogen and methanol fuels, J. Membr. Sci. 185 (2001) 29–39.

[12] P. Choi, R. Datta, Sorption in proton-exchange membranes: an explanation of Schroeder's paradox, J. Electrochem. Soc. 150 (2003) E601.

[13] P. Choi, N.H. Jalani, R. Datta, Thermodynamics and proton transport in Nafion. I. Membrane swelling, sorption, and ion-exchange equilibrium, J. Electrochem. Soc. 152 (2005) E84–E89.

[14] P. Futerko, I.-M. Hsing, Thermodynamics of water vapor uptake in perfluorosulfonic acid membranes, J. Electrochem. Soc. 146 (1999) 2049–2053.

[15] J. Divisek, M. Eikerling, V. Mazin, H. Schmitz, U. Stimming, Yu.M. Volfkovich, A study of capillary porous structure and sorption properties of Nafion proton-exchange membranes swollen in water, J. Electrochem. Soc. 145 (1998) 2677–2683.

[16] Stephen J. Paddison, Reginald Paul, T.A. Zawodzinski Jr., A statistical mechanical model of proton and water transport in a proton exchange membrane, J. Electrochem. Soc. 147 (2000) 617–626.

[17] S.A. Safran, Statistical Thermodynamics of Surfaces, Interfaces and Membranes, Addison-Wesley, Reading, MA, 1994.

[18] R. Evans, U.M.B. Marconi, Fluids in narrow pores: adsorption, capillary condensation, and critical points, J. Chem. Phys. 84 (1986) 4.

[19] A. Morro, I. Müller, A study of swelling and collapse of polyelectrolyte gels, Rheol. Acta 27 (1988) 44–51.

[20] P.J. Flory, Principles of Polymer Chemistry, Cornell University Press, Ithaca, 1953.

[21] H.B. Park, C.H. Lee, J.Y. Sohn, Y.M. Lee, B.D. Freeman, H.J. Kim, Effect of crosslinked chain length in sulfonated polyimide membranes on water sorption, proton conduction, and methanol permeation properties, J. Membr. Sci. 285 (2006) 432–443.

[22] G.M. Gusler, Y. Cohen, Equilibrium swelling of highly cross-linked polymeric resins, Ind. Eng. Chem. Res. 33 (1994) 2345–2357.

[23] V. Freger, Elastic energy in microscoically phase-separated swollen polymer networks, Polymer 43 (2002) 71–76.

[24] T.A. Zawodzinski Jr., S. Gottesfeld, S. Shoichet, T.J. McCarthy, The contact angle between water and the surface of perfluorosulphonic acid membranes, J. Appl. Electrochem. 23 (1993) 86–88.

[25] A. Bensberg, Swelling and shrinking of polyacid gels, Continuum Mech. Thermodyn. 9 (1997) 323–340.

[26] C. Heitner-Wirguin, Recent advances in perfluorinated ionomer membranes: structure, properties and applications, J. Membr. Sci. 120 (1996) 1–33.

[27] N.H. Jalani, P. Choi, R. Datta, TEOM:, A novel technique for investigating sorption in proton-exchange membranes, J. Membr. Sci. 254 (2005) 31–38.

[28] I. Müller, Thermodynamics, Pitman, Boston, MA, 1985.